

Mapping the volumetric soil water content of a California vineyard using high-frequency GPR ground wave data

Susan Hubbard, Lawrence Berkeley National Laboratory, Berkeley, California, U.S.
Katherine Grote and Yoram Rubin, University of California-Berkeley, U.S.

Water distribution in the top 1 m of the earth's surface soil layer often controls the success of agricultural crops. In this near-surface zone, large spatial and temporal variations in soil water content are associated with soil heterogeneities, topography, land cover, evapotranspiration, and precipitation. Conventional techniques of measuring soil water content for agricultural purposes—e.g., time domain reflectometry (TDR), neutron probe, or gravimetric techniques, are intrusive and provide information at a point scale only, which is often inadequate for capturing the variations in soil water content with sufficient resolution. Both passive and active remote sensing methods have also been investigated as a tool to provide soil water content in the top 0-5 cm of the sub-surface over large spatial areas and in a rapid manner. However, it is still a challenge to obtain information about soil water content from remote sensing data in the presence of a mature crop cover. At the spatial and temporal scales necessary to describe dynamic shallow soil environments, reliance on only sparse, high-resolution point measurements or on remote sensing proxy information could generate large uncertainties regarding near-surface soil water content distribution and flux.

Our research focuses on investigation of the ability of ground-penetrating radar (GPR) to provide dense estimates of shallow soil volumetric water content (VWC) in a California vineyard. Incorporation of dense, high-resolution estimates of temporal and spatial variations in soil water content could assist vineyard managers in achieving both maximum grapevine performance and irrigation efficiency. For example, variations in water availability to grapevines can lead to differences in production and quality within a vineyard block, influencing such factors as vine shoot growth, pruning weight, berry size, crop yield, sugar accumulation, titratable acidity, pH, and berry color. Grapevines can benefit from some water stress, as it forces the plant into ripening the fruit instead of putting its energy into producing more vegetation. However, major water shortages can stress grapevines, and too much water can also be damaging.

The most useful soil water content measurements for vineyard management are taken between the permanent

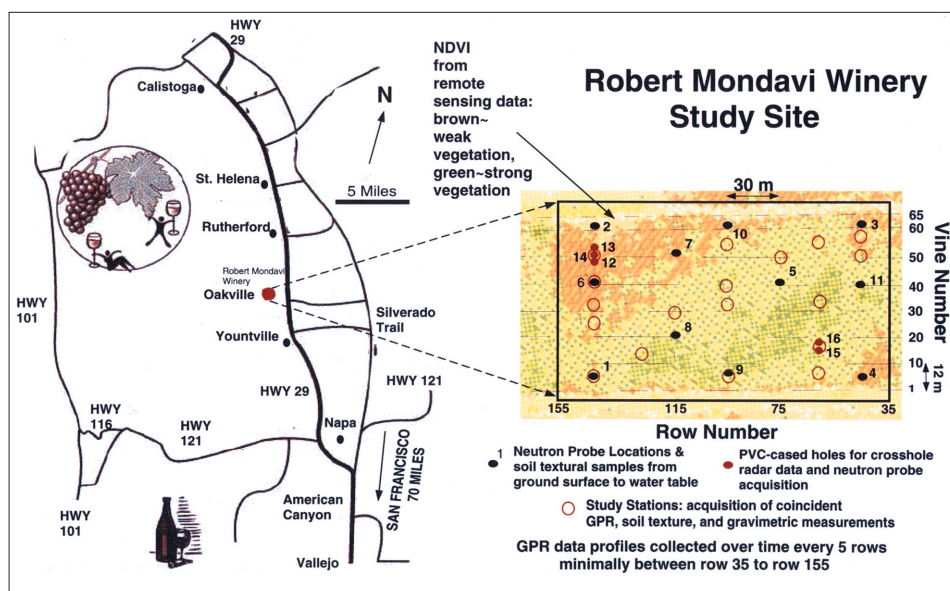


Figure 1. The x-axis is the vineyard row number, and the y-axis is the grapevine number along the row. The data grid is superimposed atop an NDVI remote-sensing image that indicates areas of weaker and more vigorous vegetation.

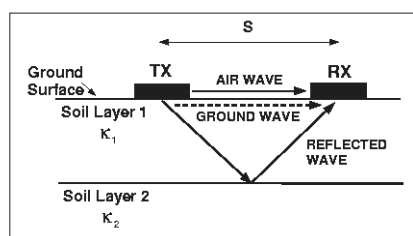


Figure 2. Air, ground, and reflected GPR energy travel paths. S is the separation distance between the transmitter (Tx) and receiver (Rx), and κ is the dielectric constant of the upper (κ_1) and lower (κ_2) geologic layers.

wilting point and the field capacity, or between VWC values of approximately 0.10-0.25. In addition to the impact of water content on grape quality and quantity, the outlay of resources and energy concomitant with crop irrigation is critical in water-scarce regions. California, which accounts for 80% of the wine grape production in the United States and has a wine grape industry valued at \$1.7 billion (California Agricultural Statistics Service, 1999), uses the largest volume of water of any state in the nation and is on the verge of a major water shortage. As vineyards consume more rural acreage, competition for water resources

is increasing. As a result, water-content information is necessary to ensure that surface water supplies do not degrade in water-scarce agricultural areas.

To test the potential of GPR to provide reliable near-surface soil water content information under natural field conditions, a study site was developed at the Robert Mondavi Winery. Although our research involves investigation of variations in amplitude and traveltime of both GPR reflected waves and ground waves, in this paper we focus only on shallow soil water content estimates obtained to date from traveltimes of GPR ground waves (lateral waves that travel in the shallow soil zone and are tied to the air-ground boundary). A companion paper by Grote et al. in the May issue of *TLE* discussed the approach that we will be applying in the vineyards to estimate the soil water content of deeper layers using GPR reflected events.

Many surface geophysical methods have been used to obtain information about subsurface water content—e.g., electrical and low-frequency electromagnetic techniques can map moisture distribution and migration in the vadose

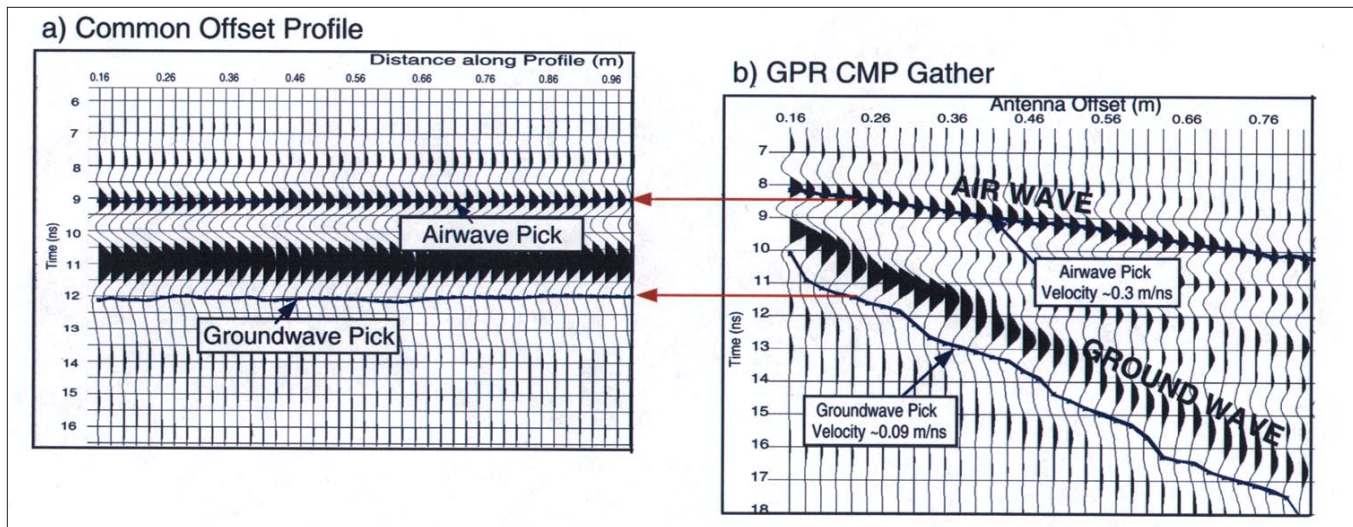


Figure 3. (a) Short section of a common-offset GPR profile showing air- and ground-wave events; (b) GPR CMP gather corresponding to common-offset profile, showing how events identified on the CMP gathers can facilitate identification of the same events on co-located common-offset data. Once the events are identified on the GPR common-offset data, they can be easily picked over the entire grid and the traveltimes differences used to estimate near-surface volumetric water content.

zone. However, these methods can be quite sensitive to the metal stakes and trellis wires used to stabilize crops, can have low spatial resolution, can be time consuming to operate, and are sensitive to temperature; therefore they are not well suited as a precision agricultural tool for rapid water content estimation. Conversely, because GPR data can be acquired rapidly and the responses are greatly influenced by water content in unsaturated materials, it could provide useful data for precision agriculture. However, to our knowledge, no previous study has analyzed spatially dense, high-resolution grids of surface GPR ground-wave data over a naturally heterogeneous agricultural site to test the feasibility of GPR as a tool to guide precision agriculture.

Data description and acquisition. The study site is next to the Robert Mondavi Winery near the town of Oakville, Napa County, California. The soils were deposited within alluvial fans, flood plains, and low terrace settings during the Holocene. The water table is approximately 3–4 m below ground surface, and the topography is fairly level. The approximately 10 000-m² site is planted with Cabernet Sauvignon grapes with row and vine spacing of 1.2 m. Mean annual precipitation in this valley is 64–89 cm. Summers are hot and dry. Winters are cool and moist with a mean annual air temperature of ~60° F. All vines in the area receive the same volume and frequency of irrigation water via a drip system—0.02 m³/vine/week during the warmest months (typically May–October). Several different types of data were collected at the site: water-content measurements using conventional sampling techniques, soil texture data, surface and cross-borehole GPR, and remote-sensing imagery.

Conventional techniques were used to measure water content at the site. These techniques provide either point measurements over some finite support scale (gravimetric) or a series of point measurements along the length of the borehole (neutron probe). Gravimetric techniques, a direct technique for estimating the total water content of the soil samples in the laboratory, is invasive, time consuming, labor-intensive, and requires laboratory equipment. However, gravimetric analysis provides direct measurements of water content, and thus is often used for calibration and verification of other indirect measurements. Soil samples were obtained at the site by hand-augering 5-cm diameter holes

into the subsurface, retrieving the samples, and quickly and carefully transporting the samples to the laboratory for gravimetric analysis.

Sixteen neutron probe access holes (Figure 1) were drilled to the water table. Soil samples were retrieved during installation of all neutron probe access tubes using a sampling interval of 30 cm. Samples were analyzed for soil gravimetric water content and converted to volumetric water content using soil and pore water density estimates of 1.65 and 1.00 g/cm³, respectively. The nongravel portions of the samples were analyzed for texture to determine percent weight of sand, silt, and clay. After retrieving the soil samples, neutron probe measurements were acquired in all access holes using a minimal vertical sampling interval of 7.5 cm. A site-specific linear calibration equation ($R^2=0.7$) was developed between the soil sample water content values and the neutron probe backscatter counts; this relationship was insensitive to soil texture.

VWC information obtained from neutron probe data was used in conjunction with crosshole radar data to investigate the relationship between dielectric constant and water content at the site. In addition to the deeper borehole soil samples used to calibrate the neutron probe readings, soil data were also collected at 18 different stations from shallow locations (less than 1 m) throughout the site during two acquisition campaigns. Soil textural analysis at our site suggests that the unsaturated section consists of a variety of soils ranging from clay to loamy sand. In the very shallow soils that are the focus of this paper (0.5 m or less), sand content ranged between 25% and 60%.

Remote sensing data sets collected annually at the Mondavi site are currently being compared with information available from soils and GPR data. The remote sensing data were acquired using the airborne ADAR Multispectral System 5500 in the blue, green, red, and near-infrared portions of the spectrum at 4300 m above ground level and with a high spatial resolution of 2×2 m. The operating frequency in this system is higher than the microwave systems typically employed to map soil moisture in areas of sparse land cover. Because plants photosynthetically absorb radiation, remote-sensing systems operating in these higher frequencies can estimate vegetation density or vigor. The response of the vegetation can be quantified using atmos-

pherically corrected reflectances in the red and near-infrared portions of the spectrum to yield normalized difference vegetation index (NDVI) values between -1 and 1. Pattern analysis algorithms can then be used to assign vegetation classifications to the data. Color variations on the NDVI imagery (Figure 1) indicate areas of weaker (brown) and more vigorous (green) vegetation. Given similar agricultural parameters and practices (such as rootstock, trellis type, row and vine spacing, and irrigation), variations in NDVI within a single crop block may indicate that the vegetation is controlled by soil heterogeneities. Indeed, a key reason that we chose to work at this site was the within-block variations on the NDVI imagery (Figure 1).

GPR data were collected during each acquisition campaign. Three acquisition geometries were used. The common offset mode was most widely used. With this mode, transmitter and receiver are a fixed distance apart (Figure 2), and the entire unit is pulled along the ground surface. With the common midpoint (CMP) acquisition mode, the transmitter and receiver are moved away from each other in fixed increments, starting with the transmitter and receiver juxtaposed and ending with an antennae separation distance of up to a few meters. GPR CMP data can be interpreted to yield information about the 1D electromagnetic velocity structure midway between the transmitter and receiver. Finally, zero offset cross-borehole radar data were also collected and compared to borehole neutron probe water-content information to investigate the site-specific petrophysical relationship between dielectric constant and water content.

For all GPR acquisition geometries, the traveltime of the recorded signal can be converted into velocity if the distance of the travel path is known or can be estimated. For example, if the depth to a GPR reflector is known, it can be used with the two-way GPR signal traveltime to estimate an average velocity of the material above the reflector. Additionally, electromagnetic wave velocities can be calculated using variable offset CMP GPR in a procedure analogous to seismic CMP data analysis. In this study, we attempt to use GPR common-offset ground-wave traveltime data to map spatial and temporal soil water content variations because this is the easiest and quickest GPR acquisition mode. To determine the traveltime of the ground wave, we must calculate the time difference (Δt) between pulse initiation and the arrival of the GPR ground wave. Because the signal travels through the GPR electronics prior to being transmitted from the antenna, it is often difficult to definitively locate the pulse initiation time in the recorded signal. Instead, we pick the arrival time of the air wave, which is a clear event, and correct back to an estimated pulse initiation time by subtracting the time that it took the electromagnetic signal to travel from the transmitting to the receiving antenna at the velocity of electromagnetic waves in air (or the speed of light). After we have calculated for each trace, we can estimate the velocity of the ground wave (V) using the separation distance associated with the transmitter and receiver (S , see Figure 2):

$$V = \frac{S}{\Delta t} \quad (1)$$

At the high frequencies typically used for surface GPR acquisition, and in geologic environments amenable to radar acquisition, the electromagnetic wave velocities obtained from (1) can be converted to dielectric constants (κ) using (Davis and Annan, 1989):

$$\kappa \approx \left(\frac{c}{V} \right)^2 \quad (2)$$

This approximation is valid for high frequencies in low-loss

materials, such as those not dominated by the presence of expanding clays or saline fluids.

Dielectric constants vary as a function of water content, porosity, operating frequency, lithology, temperature, pore fluid composition, and microgeometry. Under natural conditions, however, water content typically has the greatest influence on the measured dielectric constant of unsaturated soils. The dielectric constant of air is 1, of water is 80, and of dry natural geologic materials is 4-8; addition of water to the soil pore space drastically increases the dielectric constant and thus alters the traveltime of the GPR signal. Petrophysical models are necessary to correlate the dielectric constant estimates, available from GPR data, to water content. These petrophysical relationships can be developed for the specific site of interest or taken from the literature if available. For example, Topp et al. (1980) developed an empirical relation at the laboratory scale between dielectric constant measurements made using TDR techniques and volumetric water content:

$$VWC = -5.3 \times 10^{-2} + 2.92 \times 10^{-2} \kappa - 5.5 \times 10^{-4} \kappa^2 + 4.3 \times 10^{-6} \kappa^3 \quad (3)$$

This relationship, which suggests that an increase in dielectric constant corresponds to an increase in water content, has been widely used by soil scientists for converting measured dielectric constant values, obtained using TDR techniques, into VWC estimates. Recently, researchers have also successfully invoked the Topp relation for converting dielectric constant values from GPR data into estimates of moisture content.

GPR data analysis. Detailed studies and full field grid GPR data acquisition campaigns were performed within the Mondavi site. The detailed studies were used to develop a ground wave interpretation procedure and to investigate the accuracy of the water content estimates obtained from GPR ground wave data. The detailed studies were used in interpretation of the full field grid studies needed to investigate temporal and spatial variations in near-surface soil water content over the entire site. Detailed studies included GPR imaging during infiltration tests to assess the influence of moisture on GPR ground wave traveltimes and amplitudes, crosshole radar data acquisition for petrophysical relationship investigation, comparison of GPR signatures with soil information obtained along excavated trenches, and comparison of collocated CMP and common offset GPR data with conventional soil moisture and soil texture measurements to assess the reliability of GPR data for soil water content estimation.

A petrophysical relationship is necessary to convert the dielectric constant estimates obtained from GPR ground wave traveltime data (using equations 1 and 2) into estimates of water content. A site-specific petrophysical relationship was investigated at the Mondavi site using crosshole radar and neutron probe data. Crosshole radar data at 200 MHz were collected between two well pairs. The crosshole radar traveltime measurements and the known distances between the acquisition boreholes were used in equation 2 to calculate average dielectric constants as a function of depth between those well pairs. The field-scale petrophysical relationship was investigated by comparing the average dielectric constant values with the corresponding wellbore neutron probe water content measurements. In spite of differences between the measurement frequencies, measurement directions, and sampling volumes, our developed field-scale site-specific relationship turned out to be similar to the laboratory-derived relationship in equation 3. We are also currently investigating the site-specific relationships between dielectric constant and water content at the laboratory scale using TDR mea-

Basic facts

GPR has become increasingly popular as researchers in a variety of disciplines strive to better understand near-surface conditions. GPR uses electromagnetic energy at frequencies of 50-1500 MHz to probe the subsurface. At these frequencies, dielectric properties, characterized by the separation (polarization) of opposite electric charges within a material subjected to an external electric field, dominate the electrical response. In general, GPR performs better in unsaturated coarse- or moderately coarse-textured soils. A GPR system consists of an impulse generator which repeatedly generates a pulse of fixed voltage and frequency that propagates from the transmitting antenna through the earth. This signal is reflected, scattered, and attenuated back to the receiving antenna by subsurface dielectric contrasts. At early times in the GPR signal propagation, spherical wavefronts propagate into the ground. Because the electromagnetic velocities of air and ground are different, boundary waves are created when the spherical waves intersect the ground surface. A ground wave is formed that travels along the air-ground interface.

Figure 2 is a simple illustration of the typical energy arrivals recorded by the GPR receiving antenna (Rx) from a transmitting antenna (Tx), including the path that the energy takes in air between the transmitter and receiver, the path of the ground wave traveling along the air-ground interface, and the path of a reflected event from an interface between materials having different dielectric constant (κ) values. The paper focuses on information obtained from the ground wave traveltime data. The ground wave propagates through the top subsurface soil with a velocity dictated by the dielectric constant of that soil. The soil zone of influence is a function of the acquisition parameters and the signal wavelength (and thus the electromagnetic velocity). Lower frequency signals sample a thicker soil zone than higher frequency signals, and the soil zone of influence is thicker in drier times (when the electromagnetic velocities are higher) than in wetter times.

surement of soils having different textures. Because the lab-scale investigation is still in progress and the field-scale relationship suggested that the Topp relationship was a reasonable model for our site, all following estimates of water content from dielectric constant measurements will invoke the established empirical polynomial fit given in equation 3.

To estimate water content using the velocity of the ground wave, it is imperative to correctly identify the arrival time of the GPR air and ground waves (to enable calculation of in (1)). To assist in establishing our event-picking procedure, small-scale infiltration studies investigated the air- and ground-wave signatures and event superposition on common-offset data as a function of water content and GPR measurement frequency. Although our field studies used common offset GPR data, CMP gathers were also collected during the field campaigns to facilitate identification of the air- and ground-wave arrivals on the common-offset data. Because the slope (time vs. distance) of the air and ground wave events are distinct on CMP gathers, analysis of CMP data permits

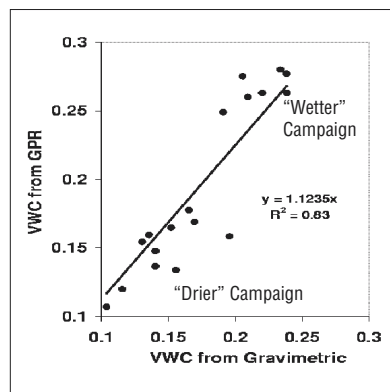


Figure 4. Comparison of shallow soil VWC values, measured at various study station locations throughout the site using gravimetric techniques, and estimated at the same locations using 900-MHz ground-wave GPR common-offset data. This figure suggests the potential of common-offset GPR ground wave data for providing accurate estimates of near-surface soil moisture.

identification of the air- and ground-wave arrivals at various antenna separation distances. When the antennas are very close together and especially when the near-surface soil is very dry (and thus the ground-wave velocity fast), the air and ground events can superimpose, rendering it challenging to pick the air and ground wave arrivals on common-offset profiles without comparison of the signatures with CMP data. Although superposition of the air and ground waves can be minimized by collecting common offset GPR data with a wider antenna separation, high-frequency GPR signals within loamy soils common to agriculture sites are subject to attenuation, thereby limiting the maximum antennae separation distance. Figure 3a shows air and ground arrivals on a GPR common offset profile and Figure 3b the corresponding CMP gather. On the CMP gather, air- and ground-wave events are easily recognizable by their linear arrivals (as a function of antenna offset distance and time) and by their velocities. This figure illustrates how air- and ground-wave signatures can be identified on the CMP gather at the separation distance associated with the common offset data (in this case, at 25 cm), and the picks can then be translated onto the common-offset profiles. However, at drier times than that associated with Figure 3a, the air and ground wave events may superimpose at the same common offset antennae separation distance. In this case, by picking a portion of the wavelet not affected by superposition and applying a correction factor to compensate for picking a traveltime point on the wavelet other than the main peak or trough, partially superimposed common offset GPR air and ground wave events can still be used to calculate Δt .

Several stations were established to investigate the thickness of the soil zone of influence on the ground wave velocity, the accuracy of the GPR common offset water content estimates, and the relationships between soil moisture and soil texture at our site. Within these stations we collected 1-m GPR common offset profiles and corresponding CMP gathers centered along the 1-m profile. In the middle of the 1-m stations, soil samples had an approximate volume of 450 cm³ for subsequent gravimetric water content and textural analysis. Data were collected under drier conditions in September 2001 and at different stations during wetter near-surface soil conditions in November 2001. VWC values estimated from GPR CMP data and calculated from gravimetric measurements compared favorably with an almost one-to-one linear relationship and an R^2 of 0.82. However, acquisition of GPR CMP data is time consuming and thus ill suited for practical water content monitoring. What is desirable is an accurate estimate of VWC using the faster GPR common offset acquisition mode. Figure 4 shows the relationship between VWC values obtained from common offset 900-MHz GPR data and VWC values from gravimetric analysis of shallow soil samples collected during both the dry and wet acquisition cam-

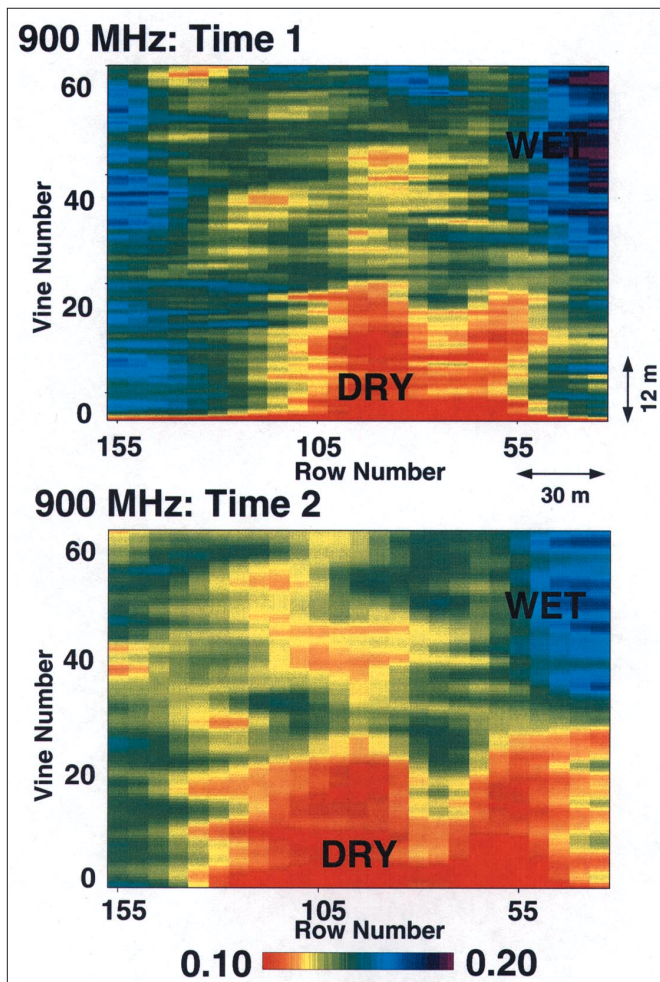


Figure 5. Comparison of volumetric water content estimates from 900-MHz common-offset GPR ground-wave data over the entire study area shown in Figure 1 during two different times of the year. These images reveal a persistence of near-surface water content spatial distribution at the site, which we interpret to be controlled by near-surface soil texture.

paings. Although the correlation in Figure 4 suggests that during drier times the GPR slightly underestimates water content and at wetter times the GPR slightly overestimates water content, the good overall correlation (R^2 of 0.83) implies that meaningful estimates of VWC can also be obtained using GPR common offset ground-wave data and that the ground wave zone of influence is similar to the depth range of the soil samples, or ~0-20 cm. This is important, as it suggests that common-offset ground-wave data, which are easy and fast to acquire, can provide dense estimates of shallow soil water content.

Investigation of the relationship between measured VWC and the percent of sand content of the corresponding samples showed a good negative linear relationship, suggesting that soils having lower sand content (and thus more silt and clay) are typically wetter than those soils having a higher percent sand content, where drainage is facilitated. However, this relationship may not hold true for deeper soils, because the water holding capacity of the soil layers located above them will also influence their moisture content.

The detailed studies suggest that, despite the differences between the support scales of the GPR and point measurements and assumptions made in converting GPR velocities into water-content estimates, common-offset GPR provides high-resolution estimates of near-surface water content in a rapid and noninvasive manner.

To enable mapping of spatial and temporal variations in near-surface water content, we analyzed ground-wave arrivals from several common offset full field grids collected during a 15-month period over the entire site. During each data acquisition campaign, GPR lines were collected along every fifth row (minimally) between rows 35 and 155 (Figure 1) using 10- or 20-cm station spacing and by stacking the data at each station 16-32 times to improve the GPR signal-to-noise ratio. GPR grids were collected during different field campaigns using multiple frequency antennas (225-, 450-, 900-, and 1200-MHz). Each grid contained approximately 20 000 GPR traces. Full field grids of 900-MHz data were collected during each campaign; the sampling interval of the 900-MHz data was 100 picoseconds. Processing all common-offset ground-wave data grids for traveltimes was minimal and included bandpass filtering and amplitude balancing.

Traveltimes associated with the GPR common-offset ground waves were picked on all data grids and converted into velocities using equation 1 with a distance (S) associated with the antenna separation for our system. The velocity values were in turn converted into dielectric constants using equation 2 and then into VWC using equation 3. A small subset of data grids are used here to illustrate results of the common-offset GPR water-content estimation procedure. Figure 5 compares VWC estimates using two different 900-MHz data grids, both collected over the entire site. These grids were collected during the warm and dry seasons; the lower grid was collected 10 months after the upper grid. The dense VWC estimates using the high-resolution GPR data (~20 000 values for each grid) were smoothed by averaging the nearest eight measurements around each sample value. Comparison of these two figures reveals a spatial persistence of near-surface water content. For example, the 900-MHz GPR common-offset data consistently reveal a drier area in the south central portion of the area, and a wetter area in the northeast. The distribution of shallow soil textures throughout the site and the relationship associated with a single acquisition campaign suggest that the near-surface water content patterns are controlled by shallow soil texture. The wetter areas correspond with shallow soil textures having a greater component of silt and clay, but the drier areas correspond with textures having a greater fraction of sand. Analysis of lower frequency GPR data grids revealed similar (although not identical) patterns of VWC but different mean VWC values than with the corresponding 900-MHz grids. This suggests that integration of multiple-frequency GPR common offset data grids, collected at the same location during the same acquisition campaign, can yield estimates of vertical and horizontal distribution of VWC.

Summary. Common-offset GPR ground-wave data can provide high-resolution estimates of shallow soil VWC within a naturally heterogeneous site. This study establishes the utility of GPR as a quick and noninvasive field tool for shallow soil water content estimates as a function of space and time. The study initially entailed detailed analysis of collocated data, with electromagnetic velocity estimates from GPR data compared to gravimetric measurements of water content and to soil texture. The detailed studies suggested that the GPR groundwave velocity data, acquired using both CMP and common offset modes, could provide accurate information about near subsurface soil water content, and that the shallow soil water content measurements were influenced by soil texture. Using the procedures developed during the detailed studies, full grids of GPR data were collected over the entire site several times during the year and analyzed to provide spatial and temporal estimates of volumetric water content. Using a subset of the GPR data grids, interpreted 900-MHz GPR grids

revealed consistent spatial patterns of shallow soil water content over time. The water-content patterns are interpreted to be associated with soil texture; the drier zones are associated with sandier near subsurface soil textures, and wetter zones with finer-grained soils. Comparison of lower-frequency GPR grids with the 900-MHz grids also revealed similar spatial patterns of volumetric water content, although the mean values varied with frequency. This suggests that incorporation of multiple frequency GPR grids can provide high-resolution estimates of soil water content variations as a function of depth as well as space and time.

Use of GPR data for providing dense soil volumetric water-content estimates can improve precision vineyard management and increase water savings in agricultural applications. The GPR water-content estimation procedure described here could also provide input to constrain vadose zone, ecological, and climate models.

Suggested reading. "Subsurface moisture determination with the ground wave of GPR," by Berkthold et al. (Proceedings, GPR 98 Conference). California Agricultural Statistics Service, Grape Crush Rpt., www.nass.usda.gov/ca/bul/crush/indexgcb.htm, 1999. "Soil water content determination using a digital ground-penetrating radar" by Chanzy et al. (*Soil Science Society of America Journal*, 1996). "Ground penetrating radar for high-resolution mapping of soil and rock stratigraphy" by Davis and Annan (*Geophysical Prospecting*, 1989). "Reconnaissance studies of moisture in the subsurface with GPR" by Du and Rummel (in Fifth International Conference on GPR, Waterloo, Kitchener, Ontario, Canada, 1994). "Velocity variations and water content estimated from multi-offset ground penetrating radar" by Greaves et al. (*GEOPHYSICS*, 1996). "GPR monitoring of volumetric water content in soils applied to highway construction and maintenance" by Grote et al. (*TLE*, 2002). "Ground penetrating radar for saturation and permeability estimation in bimodal systems" by Hubbard et al. (*Water Resour. Res.*, 1997). "Estimation of permeable pathways and water content using tomographic radar data" by Hubbard et al. (*TLE*, 1997). "Soil water content measurements at different scales: Accuracy of time domain reflectometry and ground penetrating radar" by Huisman et al. (*Journal of Hydrology*, 2001). "Remote sensing applications to hydrology: Soil moisture" by Jackson et al. (*Hydrological Sciences*, 1996). "Toward the improved use of remote sensing and process modeling in California's premium wine industry" by Johnson et al. (Proceedings IEEE International Geoscience and Remote Sensing Symposium, vol. 1, 2000). "Terrain permittivity mapping: GPR measurements of near-surface soil moisture, in proceedings on the application of geophysics to engineering and environmental problems" by Lesmes et al. (EEGS, Oakland, CA, March 1999). "Electromagnetic determination of soil water content: Measurements in coaxial transmission lines" by Topp et al. (*Water Resources Res.*, 1980). "Ground penetrating radar for determining volumetric soil water content: Results of comparative measurements at two sites" by Van Overmeeren et al. (*Journal of Hydrology*, 1997). **TLE**

Acknowledgments: This study was funded by WRC project W-929, NSF EAR-0087802, and USDA 2001-35102-09866 to Yoram Rubin. We sincerely thank Daniel Bosch and the Robert Mondavi Winery for providing vineyard technical information and vineyard access as well as in-kind support. We also thank Lee Johnson (CSU Monterey Bay and NASA/Ames Research Center) for providing access to the remote sensing imagery, and to the many researchers who participated in our field data acquisition campaigns.

Corresponding author: sshubbard@lbl.gov